Eur. Phys. J. B **21**, 175–183 (2001)

THE EUROPEAN PHYSICAL JOURNAL B

EDP Sciences

The case for universality of the phase diagram of the Fabre and Bechgaard salts

H. Wilhelm[1,a], D. Jaccard[1], R. Duprat[2], C. Bourbonnais[2], D. Jérome[3], J. Moser[3], C. Carcel[4], and J.M. Fabre[4]

[1] Département de Physique de la Matière Condensée, Université de Genève, Quai Ernest-Ansermet 24, 1211 Geneva 4, Switzerland
[2] Centre de Recherche sur les Propriétés Électroniques de Matériaux Avancés, Département de Physique, Université de Sherbrooke, Sherbrooke, Québec J1K 2R1, Canada
[3] Laboratoire de Physique des Solides[b], bâtiment 510, Université de Paris-Sud, 91405 Orsay, France
[4] Laboratoire Hétérochimie des Matériaux Organiques ENSCM/ESA-5076, 34296 Montpellier Cedex 5, France

Received 10 January 2001

Abstract. We report the observation of superconductivity in the spin-Peierls Fabre salt $(TMTTF)_2PF_6$ from pressure dependent electrical transport measurements above a threshold of 4.35 GPa. The data complete the sequence of ground states of this compound in the temperature and pressure plane adducing an empirical basis to the universal character of the phase diagram of the Fabre salts and their selenide analogues, the Bechgaard salts. The structure of the phase diagram at the approach of the crossover between spin-density wave and superconducting states is compared with the results of scaling theory of the interplay between both electronic instabilities under pressure. The comparison supports the view that magnetism and superconductivity in these compounds have a common electronic origin.

PACS. 67.55.Hc Transport properties – 71.10.Pm Fermions in reduced dimensions (anyons, composite fermions, Luttinger liquid, etc.) – 74.20.Mn Nonconventional mechanisms (spin fluctuations, polarons and bipolarons, resonating valence bond model, anyon mechanism, marginal Fermi liquid, Luttinger liquid, etc.) – 62.50.+p High-pressure and shock-wave effects in solids and liquids

1 Introduction

In the course of the last two decades that have followed the discovery of organic superconductivity in the Bechgaard salts $(TMTSF)_2X$ series [1], the study of the sulfur analog compounds − the Fabre salts $(TMTTF)_2X$ series − proved to be of equal importance in the complex task of explaining the origin of various electronic states in quasi-1D organic metals [2]. The striking complementarity and unity shown by these compounds when either hydrostatic or chemical pressure (S/Se atom or anion $X = PF_6$, AsF_6, Br, ..., substitutions) is applied, indicated from the start that their electronic and structural properties can naturally merge into a universal phase diagram [3–7]. Its content and structure came out from a cumulative experimental evidence in favour of a characteristic sequence of ground states enabling compounds of both series to be linked one to another [8–18]. In this way, Mott insulating and charge-ordered sulfur compounds like *e.g.*, $(TMTTF)_2PF_6$ or $(TMTTF)_2AsF_6$ were found to develop a lattice distorted spin-Peierls (SP) state which is suppressed under moderate pressure and replaced by an antiferromagnetic (AF) Néel state similar to the one found in the $(TMTTF)_2Br$ salt at normal conditions; the Mott state becomes in its turn suppressed under pressure and antiferromagnetism of sulfur compounds then acquires an itinerant character analog to the spin-density wave (SDW) state of the $(TMTSF)_2X$ series at low pressure. Around some critical pressure p_c, the SDW state is then removed as the dominant ordering and forms a common boundary with superconductivity which closes the sequence as the far end ordered state.

Although important pieces of the sequence has received sound experimental backing so far, the observation of the whole spectrum of states within a single compound like $(TMTTF)_2PF_6$ remained until now conjectural. Putting this amazing possibility on empirical grounds is not only a clear-cut objective from the experimental point of view [11,17], but it is also of primary concern from the standpoint of their description since it allows to broaden the follow-up of various instabilities for both electron and phonon systems which is essential in the

[a] *Present address*: Max-Planck-Institut für Chemische Physik fester Stoffe, Nöthnitzerstr. 40, 01187 Dresden, Germany
e-mail: `wilhelm@cpfs.mpg.de`
[b] associé au CNRS

determination of the conditions leading to unconventional pairing in these organic materials.

The efforts undertaken in this work aimed at establishing the conditions that lead to superconductivity in the spin-Peierls compound $(TMTTF)_2PF_6$ under the light of both experiment and theory. On the experimental ground, we studied the longitudinal electrical resistivity ρ_a as a function of temperature (T) and pressure by using a piston-cylinder clamped cell and a Bridgman pressure cell. At a pressure of 4.35 GPa, we observed superconductivity at $T_c = 1.8$ K [19,20]. Above that threshold, the pressure profile of T_c is similar to other compounds like $(TMTSF)_2PF_6$ and $(TMTSF)_2AsF_6$ above 0.9 GPa [1] and 1.2 GPa [9], respectively, or $(TMTTF)_2Br$ above 2.6 GPa [13], establishing in this way the genuine universality of the phase diagram of the $(TM)_2X$ family.

The point at issue for the theoretical description mainly concerns the influence exerted by the precursors of the transition on the emergence and the nature of superconducting pairing. The data indicate at the outset that strong SDW correlations are still tied to the onset of superconductivity in $(TMTTF)_2PF_6$ and expand far into the normal phase − a finding consistent with the pronounced enhancement of the NMR spin-lattice relaxation rate seen above the superconducting phase of $(TMTSF)_2X$ [12]. The close proximity of antiferromagnetism to superconductivity together with a normal phase dominated by spin fluctuations not only indicates that Coulomb repulsion plays a predominant role among interactions but also that both instabilities of the normal state cannot be considered as independent and interfere with each other. Owing to the pronounced metallic character of these compounds near p_c, the interference can be seen to originate in the interdependence of scattering events between electrons and holes, namely those that make up the elementary Cooper and Peierls (staggered density-wave) pairings close to the Fermi surface. In this work we will adopt a purely electronic standpoint in the description of interference calling on a recent application of scaling concepts for that problem [21]. The comparison of theory with experimental findings in $(TMTTF)_2PF_6$ near p_c confirms that superconducting pairing occurs between electrons on neighbouring stacks [4,22,23] and supports the idea that both SDW and superconductivity phenomena in such systems have a common origin.

This paper is organized as follows: in Section 2 the experimental results of the electrical transport investigation on $(TMTTF)_2PF_6$ under pressure and the phase diagram are presented. Section 3 is devoted to a qualitative comparison between scaling theory and experiments. The possibility of reentrant superconductivity in the crossover region and the limitations of the conventional electron-phonon mechanism are discussed. We conclude this work in Section 4.

2 Experimental results

The electrical transport measurements on $(TMTTF)_2PF_6$ were performed either with a piston-cylinder clamped cell

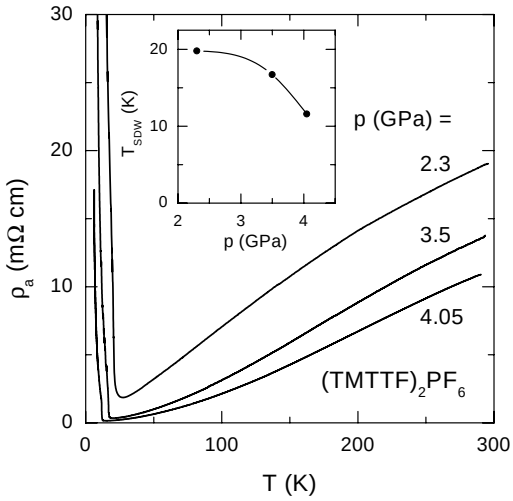

Fig. 1. Temperature dependence of the longitudinal resistivity ρ_a of $(TMTTF)_2PF_6$ obtained in the piston-cylinder clamped cell, inset: pressure dependence of T_{SDW} (see text).

($p_{max} \approx 4$ GPa) or a Bridgman anvil cell ($p_{max} \approx 10$ GPa). Technical details of the latter device can be found in reference [24] and a thorough presentation of the results is given in reference [19]. Here additional aspects of the experiments not mentioned in reference [19] are given. The longitudinal electrical resistivity $\rho_a(T)$ studied with the piston-cylinder clamped cell is shown in Figure 1. As a function of temperature ρ_a decreases monotonously upon cooling to temperatures of the order of 10 K. In this temperature regime, ρ_a passes through a minimum at T_{min} and the upturn in $\rho_a(T)$ is related to a transition into an insulating state, attributed to the onset of itinerant antiferromagnetism at T_{SDW} [17,24]. Pressure rapidly suppresses T_{SDW} (inset Fig. 1) and the extrapolation of $T_{SDW}(p)$ for $T \to 0$ predicts the formation of a metallic state for 4.5 ± 0.1 GPa. Access to this pressure region is provided by the Bridgman anvil cell. The resistivity $\rho(T)$ of a single crystal from the same batch measured at 3.7 GPa showed a similar low temperature behaviour as the sample used in the piston-cylinder clamped cell. Thus, we are confident that the combination of the results of the two experiments is on firm grounds. The strong increase of $\rho(T)$ below 20 K is disrupted by the onset of a sharp drop in resistivity at $T_c = 1.8$ K ($p = 4.35$ GPa) as shown in the inset of Figure 2. The drop in resistivity is more pronounced at slightly higher pressure (main part of Fig. 2). At 4.73 GPa the resistivity starts to decline at $T_c = 2.2$ K and has decreased by one order of magnitude at 1 K. Upon pressure increase T_c as well as the magnitude of the drop in resistivity decrease further. Beyond 7 GPa no evidence of a drop in resistivity was found. A strong argument to identify T_c as a superconducting transition temperature is provided by the influence of an external magnetic field applied along the c-axis [19].

The resistivity data obtained in the two pressure devices differ in two points. Firstly, in the Bridgman anvil cell the metallic coherence is much less developed at low temperature, and secondly a maximum occurred in the

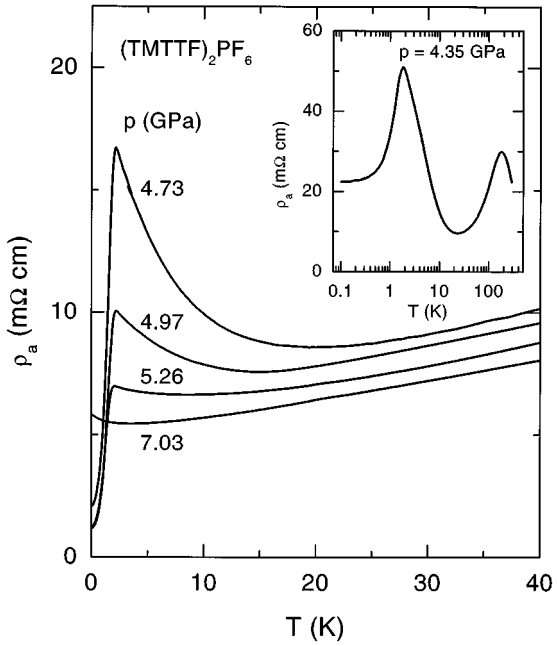

Fig. 2. Electrical resistivity $\rho(T)$ of $(TMTTF)_2PF_6$ at various pressures and low temperature, obtained using the Bridgman anvil cell. Inset: $\rho(T)$ below 300 K at $p = 4.35$ GPa in a semilogarithmic scale.

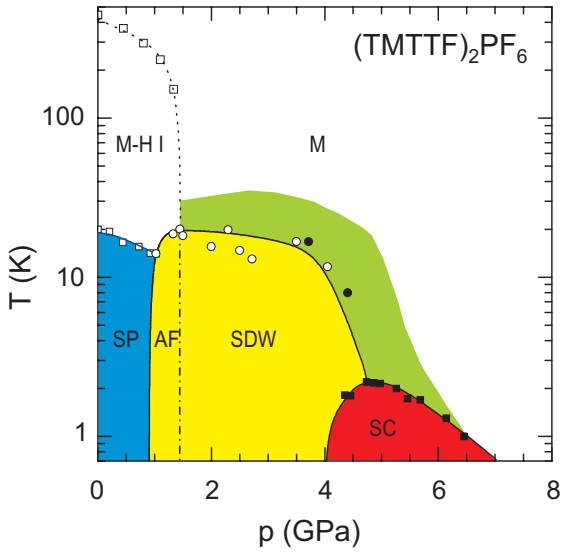

Fig. 3. (T, p) phase diagram of $(TMTTF)_2PF_6$. The spin-density wave (SDW) state is suppressed and a superconducting (SC) phase emerges above 4 GPa. Over a wide pressure range AF fluctuations (emphasized region in the M state) are present. A Mott-Hubbard (M-H I) insulating and a metallic (M) state are present at high temperature, SP denotes the spin-Peierls state. Open symbols represent data taken from reference [17].

high temperature domain of $\rho(T)$ in the vicinity of 200 K (inset Fig. 2). Such a maximum was not observed using the piston-cylinder clamped cell (Fig. 1) nor in several previous experiments performed with the Bridgman anvil cell. We attribute these discrepancies to the peculiar pressure conditions in the Bridgman anvil cell: In the latter technique steatite, a soft mineral, is used as pressure transmitting medium [19]. Since $(TMTTF)_2PF_6$ is mechanically weak and extremely brittle the sample cracks easily and may rearrange slightly during the initial pressurization. As a result a transverse resistivity component $\rho_\perp$, which is about two orders of magnitude larger than ρ_a [17] influences the results in a non-negligible manner, explaining qualitatively the observations, notably the maximum in $\rho(T)$ at about 200 K. Despite these differences, we are convinced that these features do not interfere significantly with the low temperature properties and the conclusions drawn in this article.

Figure 3 comprises the low and high pressure results of $(TMTTF)_2PF_6$ and establishes the generic character of the phase diagram [19]. Here we would like to emphasize that the reentrance of superconductivity below the SDW ordering appears to be a general behaviour among $(TM)_2X$ superconductors. It has also been identified with a finite resistivity in the "superconducting" state in $(TMTSF)_2AsF_6$ [25,26].

The behaviour of the magnetoresistivity up to 8 T at 500 mK did not reveal any sign of field-induced spin-density wave (FISDW) phases, which has been observed in all Se-X compounds [27]. The existence of a non-zero threshold field H_t for the stabilisation of FISDW phases is the result of bad nesting properties of the Fermi surface along the c-direction. It is defined by the relation $t'_c = T_{FISDW}(H_t)$ [28], where t'_c is the transverse coupling between next-nearest neighbour stacks related to the deviation of perfect nesting along c and $T_{FISDW}(H)$ is the definition of the FISDW transition temperature of the 2D electron gas. For all selenide based $(TM)_2X$ conductors the ambient pressure SDW state is suppressed under rather modest pressures of about 1 GPa in $(TMTSF)_2PF_6$, $(TMTSF)_2ReO_4$ and even at ambient pressure in the relaxed state of $(TMTSF)_2ClO_4$ [29]. The calculated coupling between neighbouring stacks along the c-direction is small, $t_c = 2$ meV ($t'_c \ll t_c$) and independent of the nature of the organic molecule, *i.e.*, TMTTF or its selenide analogue TMTSF [13,30]. Therefore, we can infer that a pressure of 4.5 GPa might be large enough to significantly raise the value of t'_c above its ambient pressure value ($t'_c = 0.043$ meV) [29]. Hence, the condition $t'_c = T_{FISDW}(H_t)$ could no longer be fulfilled at fields H lower than 8 T. Also in $(TMTTF)_2Br$, which becomes superconducting at 2.6 GPa [13], no FISDW could be detected below 8 T (although a threshold field may be located around 13 T) [31]. Therefore, the higher pressure necessary to induce superconductivity in $(TMTTF)_2PF_6$ is consistent with the situation encountered previously in $(TMTTF)_2Br$, namely the onset field might be larger than 8 T.

3 Theory and experiment

This section gives a brief account of the contribution of scaling theory to the problem of interplay between SDW

and superconducting correlations in quasi-1D metals. Carried out in the framework of a quasi-1D electron gas model, scaling theory is at the outset a weak coupling approach that points out the qualitative features of this complex issue, but which may throw light on what does occur in systems like $(TMTTF)_2PF_6$ at high pressure.

3.1 Scaling theory

We assume in the following that the mutual interaction between itinerant antiferromagnetism and superconductivity in metallic systems like $(TMTTF)_2X$ and $(TMTSF)_2X$ at high and moderate pressure, respectively, has a purely electronic origin and that phonons are not involved (see Sect. 3.3). We thus focus our attention on those interacting quasi-particles close to the Fermi surface whose warping is supposed to describe coherent electronic motion along two spatial directions below some characteristic energy scale. As for the influence of higher energy states appertaining to the 1D non-Fermi-liquid physics, it can be accounted for by the renormalization group method. This procedure is carried out in the 1D energy domain by integrating out electron and hole states from the band edge of isolated chains down to the energy $\pm E_x/2$ from the Fermi surface, which marks the onset of inter-chain coherent motion [32]. The effective low-energy Hamiltonian then takes the form

$$H^* = \sum_{r,\sigma} \sum_{\{\mathbf{k}\}^*} E_r^*(\mathbf{k})\; a^\dagger_{r,\mathbf{k},\sigma} a_{r,\mathbf{k},\sigma} + H_{\rm I}^*, \qquad (1)$$

where

$$E_r^*(\mathbf{k}) = v_{\rm F}(rk - k_{\rm F}^0) - 2t_b^* \cos(k_\perp d_\perp) - 2t_{b2}^* \cos(2k_\perp d_\perp)$$

is the quasi-particle spectrum for right ($r = +$) and left ($r = -$) moving carriers along the chains, $v_{\rm F}$ is the longitudinal Fermi velocity, and $d_\perp$ is the inter-chain distance, whereas t_b^* and t_{b2}^* are the effective inter-chain hopping to first- and second-nearest neighbour chains, respectively. The latter acts as a small perturbation which will serve to parametrize nesting deviations of the Fermi surface [33]. The inter-chain hopping t_b^*, which is directly related to the amplitude of the warping of the Fermi surface, then fixes the cut-off energy scale for inter-chain coherence, namely $E_x \approx t_b^*$. The essential contributions to the effective electron-electron interaction that defines $H_{\rm I}^*$ at E_x are found to be

$$H_{\rm I}^* = \frac{\pi v_{\rm F}}{LN_\perp} \sum_\mu \sum_{\{\mathbf{k},\mathbf{k}',\mathbf{Q}\}^*} \sum_{\alpha\beta\gamma\delta} J_\mu(q_\perp) \big(a^\dagger_{+,\alpha}(\mathbf{k}+\mathbf{Q})\, \sigma_\mu^{\alpha\beta}\, a_{-,\beta}(\mathbf{k})\big) \times \big(a^\dagger_{-,\gamma}(\mathbf{k}'-\mathbf{Q})\, \sigma_\mu^{\gamma\delta}\, a_{+,\delta}(\mathbf{k}')\big), \qquad (2)$$

which is expressed as a sum of products of electron-hole pair fields describing the contributions of coupling constants to charge-density wave (CDW) ($\mu = 0$) and SDW ($\mu = 1,2,3$) correlations. Here $\sigma_0 = \mathbf{1}$, $\sigma_{\mu=1,2,3}$ are the Pauli matrices, $\mathbf{Q} = (2k_{\rm F}^0 + q, q_\perp)$, and $N_\perp$ is the number of chains of length L. From the 1D theory, the corresponding couplings (expressed in $\pi v_{\rm F}$ units) at E_x are

$$J_\mu(q_\perp) = -g_\mu^* + j_{\perp\mu} \cos(q_\perp d_\perp). \qquad (3)$$

These contain a local repulsive part g_μ^* and an inter-chain contribution $j_{\perp\mu} > 0$, which favours out of phase inter-chain CDW or SDW correlations at the best nesting vector $\mathbf{Q}_0 = (2k_{\rm F}^0, \pi/d_\perp)$ of the spectrum $E^*(\mathbf{k})$ at low energy. For repulsive bare interactions, the results of the 1D scaling theory tell us that among the scattering amplitudes, $J_{\mu\neq 0}$ is by far the largest indicating that short-range SDW correlations are present at E_x. Their strengthening continues at lower energy and is governed in part by the electron-hole pairing response of the system enhanced by nesting. However, the same electron and hole degrees of freedom can be connected through another singular electronic response which is related to electron-electron (hole-hole) pairing involved in superconductivity. This crossed pairing also called interference between Cooper and Peierls channels is well known to be maximum in the 1D non-Fermi-liquid state at $T \gg E_x/2$, but is usually neglected at much lower temperature [3,4,22,23,34–39]. Actually, far from being irrelevant in the latter conditions, its influence became unevenly distributed along the Fermi surface, which has in turn a striking impact on the nature of long-range ordering at low temperature.

The effect of interference below E_x has recently been worked out using the renormalization group method and the main results [21] will be sketched out here. Following an infinitesimal scaling of the bandwidth $E_x(\ell) \to E_x(\ell + {\rm d}\ell) = E_x(\ell){\rm e}^{-{\rm d}\ell}$, the Hamiltonian undergoes the transformation $\mathcal{R}_{{\rm d}\ell}[H_\ell^*] \to H_{\ell+{\rm d}\ell}^*$, which leads to the renormalization or flow of its parameters. By combining both types of pairing at the one-loop level, the flow of interactions has been shown to be governed by the equations

$$\frac{\rm d}{{\rm d}\ell} J_\mu(q_\perp - k_\perp, k_\perp; \ell) = (N_\perp)^{-1} \sum_{\bar\mu, k'_\perp} c_{\mu,\bar\mu} W_{\bar\mu}(q_\perp - k_\perp, k'_\perp; \ell) W_{\bar\mu}(k'_\perp, k_\perp; \ell) I_{\rm C}(\ell) - J_\mu(q_\perp - k_\perp, k_\perp; \ell)\, (N_\perp)^{-1} \times \sum_{k'_\perp} J_\mu(q_\perp - k'_\perp, k'_\perp; \ell)\, I_{\rm P}(q_\perp, k'_\perp; \ell), \qquad (4)$$

for CDW ($\mu = 0$) and SDW ($\mu \neq 0$) channels. The first term in the right-hand-side comes from the Cooper channel with the combinations of couplings $W_{\bar\mu=0} = -\frac{1}{2}J_0 + \frac{3}{2}J_{\mu\neq 0}$ for singlet (SS) and $W_{\bar\mu=1,2,3} = \frac{1}{2}J_0 + \frac{1}{2}J_{\mu\neq 0}$ for triplet (TS) pairings and the constants $c_{0,0} = -1/2$, $c_{0,\bar\mu\neq 0} = 1/2$ and $c_{\mu\neq 0,0} = 1/2$, $c_{\mu\neq 0,\bar\mu\neq 0} = 1/6$. In the expression (4), $I_{\rm C}(\ell) = \tanh[\beta E_x(\ell)/4]$ is the derivative of the non interacting Cooper pairing response ($\pi v_{\rm F} d\chi_{\rm C}^0/d\ell$) evaluated in the static limit and at zero pair momentum.

The Peierls counterpart is given by

$$I_{\rm P}(q_\perp,k'_\perp,\ell)=\frac{E_x(\ell)}{4}\times\sum_{r=\pm}\frac{\tanh\frac{\beta}{4}E_x(\ell)+\tanh\frac{\beta}{2}[E_x(\ell)/2+rA(k'_\perp,q_\perp)]}{E_x(\ell)+rA(k'_\perp,q_\perp)},$$

which locally defines the derivative of the electron-hole pairing response at the wavevector $(2k_{\rm F}^0,q_\perp)$ for an electron (or a hole) at $k'_\perp$ on constant energy surface at $\pm E_x/2$ from the Fermi edge. Deviations from perfect nesting are

$$A(k'_\perp,q_\perp)=2t_b^*[\cos(k'_\perp d_\perp)+\cos(k'_\perp d_\perp+q_\perp d_\perp)]+2t_{b2}^*[\cos(2k'_\perp d_\perp)+\cos(2k'_\perp d_\perp+2q_\perp d_\perp)].$$

The influence exerted by Cooper pairing terms in (4) is responsible for the emergence of a $k_\perp$ dependence in the scattering amplitudes, a dependence that was not present in J_μ at the start. Interference thus introduces non uniform electron-hole pairing which affects the properties of the SDW state as we will see. The numerical integration of (4) for repulsive couplings $g^*_{\mu\neq0}>g^*_{\mu=0}$ and $j_{\perp\mu\neq0}>j_{\perp\mu=0}$ leads to a singularity of $J_{\mu\neq0}$ in the SDW channel at finite ℓ and $q_\perp=\pi/d_\perp$. Scaling to strong coupling signals an instability of the normal state towards the formation of bound electron-hole pairs. Although a true phase transition is impossible in a strictly 2D system at finite temperature, the one-loop temperature scale $T_{\rm SDW}=E_x(\ell_{\rm SDW})/2$ for strong coupling is nevertheless indicative of the temperature domain for the onset of long-range order if for example a small but finite hopping in the third spatial direction is introduced.

The SDW temperature thus obtained is the highest when nesting deviations are absent, which occurs at $t^*_{\perp2}=0$. On practical level, if one feeds (4) by the couplings $J_{\mu\neq0}\simeq0.85$ ($J_{\mu=0}\simeq0.17$) using $E_x=120$ K as the bandwidth cut-off of the low energy theory, we find $T_{\rm SDW}\simeq13$ K, which falls in the range of observed SDW critical temperatures when pronounced metallic conditions prevail in the normal state. Although there is of course some arbitrariness in the selection of various parameters that can lead to this temperature scale, our choice is nevertheless compatible with the expected range of band parameters and coupling constants [6,12]. Besides differences in numbers, the qualitative features shown by the model at low-energy are rather generic in the repulsive sector of bare interactions.

As one approaches $\ell_{\rm SDW}$, the variation of the scattering amplitude $J_{\mu\neq0}(\pi/d_\perp-k_\perp,k_\perp;\ell)$ with $k_\perp$ reveals the existence of cold and hot spots centered at $k_\perp=\pm\pi/(2d_\perp)$ and $k_\perp=\pm\pi/d_\perp,0$, respectively, along constant energy surface from the Fermi edge $\pm k_{\rm F}(k_\perp)$, parametrized by the transverse wavevector $k_\perp$. By cold spots, we mean regions of significantly reduced scattering intensity. This uneven amplitude of electron-hole pairing above $T_{\rm SDW}$ will also be present in the variation of the SDW order parameter or the gap $\Delta_{\mu\neq0}(k_\perp)$ along the Fermi surface below $T_{\rm SDW}$.

In order to simulate the impact of pressure on the above SDW instability of the normal state, we will assume

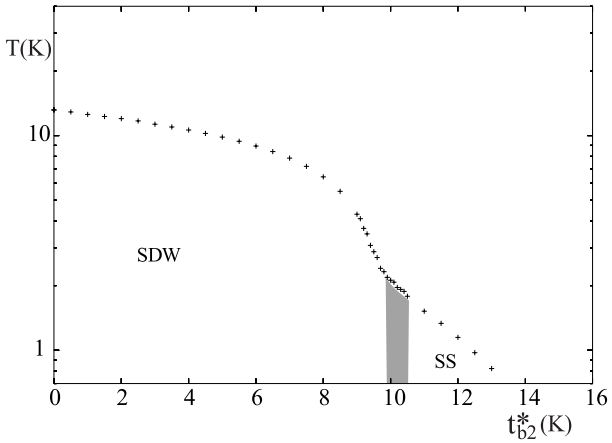

Fig. 4. Diagram of normal state instabilities calculated from the renormalization group method at the one-loop level (see text for the value of parameters used). The shaded area corresponds to the crossover region where both SDW and SS couplings scale to strong couplings.

that its influence on the crystallographic structure modifies the band parameters and in their turn the strength of electronic correlations at low energy. In the following we will adopt the simple picture where the latter effect can be entirely parametrized by t^*_{b2} which controls the growth of nesting deviations in the Peierls channel. In this way, by taking an increase of the effective cut-off $\mathrm{d}E_x/\mathrm{d}t^*_{b2}=5$ and a decrease of the strength of the couplings $\mathrm{d}g^*_{\mu\neq0}(j_{\perp\mu\neq0})/\mathrm{d}t^*_{b2}=-4\%/\mathrm{K}$ ($-4\%/\mathrm{K}$) and $\mathrm{d}g^*_{\mu=0}(j_{\perp\mu=0})/\mathrm{d}t^*_{b2}=-6\%/\mathrm{K}(-8\%/\mathrm{K})$ [40], $T_{\rm SDW}$ first gradually decreases and ultimately drops rapidly (Fig. 4). The variation of $J_{\mu\neq0}$ with $k_\perp$ magnifies along this drop entailing a similar variation of the amplitude of the SDW gap along the Fermi surface in the condensed phase. When t^*_{b2} is further increased, the critical line presents an inflection point at t^{*c}_{b2} ($t^{*c}_{b2}\approx9.8$ K, using the above set of parameters) where the structure of $J_\mu(k'_\perp,k_\perp;\ell)$ is altered and shows a singular modulation as a function of $k_\perp$ and $k'_\perp$ at a value denoted $\ell_{\rm c}$ ($T_{\rm c}=E_x(\ell_{\rm c})/2$ is the corresponding temperature scale). This marks the occurrence of a strong coupling regime which involves the superconducting channel. The connection with superconductivity can be seen by rewriting the effective interaction as

$$H^*_{\rm I}(\ell)=-\frac{\pi v_{\rm F}}{LN_\perp}\sum_{\bar\mu}\sum_{\{\mathbf{k},\mathbf{k}',\mathbf{Q}_c\}^*}\sum_{\alpha\beta\gamma\delta}W_{\bar\mu}(k_\perp,k'_\perp;\ell)\times\left(\alpha\,a^\dagger_{+,\alpha}(\mathbf{k}+\mathbf{Q}_c)\,\sigma^{\alpha\beta}_{\bar\mu}\,a^\dagger_{-,\beta}(\mathbf{k})\right)\times\left(\gamma\,a_{-,\gamma}(\mathbf{k}'-\mathbf{Q}_c)\,\sigma^{\gamma\delta}_{\bar\mu}\,a_{+,\delta}(\mathbf{k}')\right),\quad(5)$$

which is expressed in terms of products of Cooper pair fields $\sim a^{(\dagger)}_{\mp,\alpha}\,\sigma^{\alpha\beta}_{\bar\mu}\,a^{(\dagger)}_{\pm,\beta}$. The even modulation in $k_\perp,k'_\perp$ that appears at the threshold t^{*c}_{b2} is dominated by the first Fourier harmonic in the SS channel, namely $W_{\bar\mu=0}(k_\perp,k'_\perp;\ell)\approx a_0(\ell)\cos(k_\perp d_\perp)\cos(k'_\perp d_\perp)$, which gives rise to strong coupling for SS pairing between electrons on first-nearest-neighbour chains. Given

the relation $W_{\bar{\mu}=0} = -\frac{1}{2}J_0 + \frac{3}{2}J_{\mu\neq 0}$, the Cooper pairing is induced by SDW correlations, that is, the singularity in the Fourier coefficient $a_0(\ell_c)$ at ℓ_c is governed by $J_{\mu\neq 0}$ in the $k_\perp, k'_\perp$ plane. At t^{*c}_{b2}, both SDW and SS scattering amplitudes show strong coupling behaviour and accordingly, this yields the onset of critical correlations in both channels. As t^*_{b2} is further increased above the threshold, T_c gradually decreases while SDW correlations, albeit large in amplitude, see their critical behaviour suppressed so that only the SS channel remains singular. Owing to the separation of variables in $W_0(k_\perp, k'_\perp; \ell)$ mentioned above, the instability will lead to a singlet gap $\Delta(k_\perp) = |\Delta_0|\cos(k_\perp d_\perp)$ with nodes located at the cold spots $k_\perp = \pm\pi/(2d_\perp)$. The signature of an inter-chain SS instability can also be seen through the profile of electron-hole pairing $J_{\mu\neq 0}(\pi/d_\perp - k_\perp, k_\perp)$ along the Fermi surface which varies as $\cos^2(k_\perp d_\perp)$ for t^*_{b2} sufficiently above t^{*c}_{b2} as a result of interference.

The case of $(TMTTF)_2PF_6$ offers an interesting experimental backing to the previous theoretical description. Our data provide the missing information enabling the (p, T) phase diagram of $(TMTTF)_2PF_6$ presented in Figure 3 to be constructed and establish its truly universal character: The SP phase [16,41] precedes the AF (Néel and SDW) ground states which are stable up to about 4 GPa [17] and then a superconducting region extends to almost 7 GPa with $T_c = 2.2$ K at 4.73 GPa. Over a large pressure range AF spin fluctuations are present, indicated in Figure 3 by the emphasized area in the M state. The boundaries of this region, where the upturn in $\rho(T)$ is observed, are defined by $T_{\min}$ and either T_{SDW} or T_c. The width in temperature of this interval increases with decreasing pressure and is largest where $T_c(p)$ reaches its optimum value. Thus, $T_{\min}$ appears to be closely linked to the critical temperature T_c. Critical AF fluctuations seem to be enhanced when the SDW ground state is approached from high pressure, *i.e.*, when the system is close to the border of the SDW and superconducting phases. At slightly lower pressure the decrease of T_c is clearly related to the occurrence of the SDW phase at a higher temperature. A similar behaviour is encountered in the competition between CDW and superconducting instabilities in layered conductors [42]. The correlation between the fall of T_{SDW} and the rise in T_c reflects the suppression of the SDW gap with pressure. These features are in qualitative agreement with the scaling results which show a variation of the temperature scale for the instability of the normal state with t^*_{b2} that simulates fairly well the actual behaviour seen under pressure.

3.2 Reentrant superconductivity and crossover region

The above scaling results show the existence of a finite interval in t^*_{b2} where scaling to strong coupling for both SS and SDW pairings is found (shaded region in Fig. 4). Although definite predictions as to the structure of the phase diagram in this crossover region cannot be made within the present weak coupling framework, one can infer from the available information that superconductivity is likely to be the most stable state. Consider the case where the SDW instability first occurs as the temperature is lowered. According to the ansatz where the SDW gap $\Delta_{\mu\neq 0}(k_\perp) = |\Delta_{SDW}|d(k_\perp)$ will show a variation $d(k_\perp)$ similar to the scattering amplitude $J_{\mu\neq 0}(\pi/d_\perp - k_\perp, k_\perp; \ell_{SDW}) \propto d(k_\perp)$ along the Fermi surface, the SDW condensation energy will then be strongly reduced. The system has then the possibility to compete with a superconducting ordered state having a lower T_c but a gap $\Delta(k_\perp) = |\Delta_0|\cos(k_\perp d_\perp)$ that is more developed along the Fermi surface. This possibility can be illustrated by expanding the condensation energy for each ordered state in lowest order in the gap function [21]. In the zero temperature limit, one finds for the ratio of condensation energies

$$\frac{\delta E_{SDW}}{\delta E_{SS}} \approx \frac{T^2_{SDW}}{T_c^2}\,\frac{2}{N_\perp}\sum_{k_\perp} d^2(k_\perp), \qquad (6)$$

which can become smaller than unity if T_{SDW} is close to T_c and $d(k_\perp)$ is sufficiently small compared to $|\cos(k_\perp d_\perp)|$. It turns out that both conditions are essentially met in the crossover region. As pointed out by Yamaji [43], such a crossing of condensation energies would give rise to a first-order transition from SDW to SS states. According to the phase diagram of Figure 3 the reentrant line below T_{SDW} would correspond to an equilibrium curve with positive dT/dp and emission of latent heat when the system enters in the SS state. In this scenario the critical pressure (p_c, T_c) is likely to terminate the first-order line as a second-order order critical point.

An alternative scenario can be considered if the ratio of condensation energies are so close to one another that no true SDW ordered state is stabilized in the crossover region and the only phase transition to occur would be a superconducting one. Since both SS and SDW couplings scale to strong coupling in that region, superconductivity will then come out from a background of critical SDW correlations. The latter will affect the properties of the normal state, especially those related to electrical transport. These features may be equated as well with reentrant superconductivity found in $(TMTTF)_2PF_6$ (Fig. 2) and $(TM)_2X$ in general near p_c [25]. Now since SDW correlations become essentially 'soft' in this sector, strong coupling competes with dynamical (retardation) effects in the exchange of SDW correlations and may be responsible for a maximum in T_c at p_c − a similar situation is found in conventional superconductors where there is a maximum attainable T_c in the large electron-phonon coupling limit [44].

3.3 Digression on the electron-phonon coupling

The stabilization of superconductivity from a SP state in $(TMTTF)_2PF_6$ at high pressure provides an interesting opportunity to estimate the strength of the electron-phonon coupling in the sector of the phase diagram where Cooper pairing becomes favourable. The SP phase transition in $(TMTTF)_2PF_6$ is found to occur at $T_{SP} \approx 19$ K

at ambient pressure [10,41], and it is preceded by 1D precursors (lattice softening) up to about 60 K, as borne out by X-ray diffuse scattering data [10]. The SP character ascribed to both the lattice softening and the ordered state comes from the fact that at higher temperature, namely below $T_\rho \approx 220$ K [8] (Fig. 3), $(TMTTF)_2PF_6$ presents a Mott insulating behaviour and that the pseudo-gap (resp. true gap) in the *spin* sector occurs only below $T_{SP}^0 \approx 40\,\mathrm{K} \ll T_\rho$ (resp. T_{SP}) − as shown by spin susceptibility and NMR data [12,41,45]. T_{SP}^0 then marks the onset of strong coupling between 'bond' CDW correlations and acoustic phonons of wavevector $2k_F^0$. In the framework of scaling theory [6,46,47], both temperatures T_{SP}^0 and T_ρ are connected through the static electron-electron interaction induced by the exchange of $2k_F^0$ acoustic phonons, which is denoted g_{ph} in the expression

$$T_{SP}^0 = c \mid g_{ph} \mid T_\rho, \tag{7}$$

where c is a constant of the order of unity. Given the empirical values for T_{SP}^0 and T_ρ, one finds $g_{ph} \approx -0.15$ (in πv_F units) as the bare interaction induced by phonons in $(TMTTF)_2PF_6$ at ambient pressure. Thus, a small ratio for T_{SP}^0/T_ρ is congruent with an electron-phonon interaction that is weak in comparison to the Coulomb repulsion as it can be extracted from NMR data or quantum chemistry calculations ($|g_{ph}| \ll g_\mu$) [12,48].

The relation (7) is also useful to understand another key experimental finding: the suppression of the spin pseudo-gap after a sizable decrease of T_ρ (Fig. 3) − as shown by NMR in $(TMTTF)_2PF_6$ at 1.5 GPa ($T_\rho \approx$ 75 K) and $(TMTTF)_2Br$ at ambient pressure ($T_\rho \approx$ 100 K) [12,41]. Assuming an increase of the Debye frequency ω_D under pressure that overcomes the one of v_F (or t_a) in $g_{ph} \propto t_a/\omega_D^2$ by taking the reasonable variations $(1/t_a)\mathrm{d}t_a/\mathrm{d}p \sim (1/\omega_D)\mathrm{d}\omega_D/\mathrm{d}p \approx 15\%/\mathrm{GPa}$ [25] we arrive at $|g_{ph}| \sim 0.05$ for $(TMTTF)_2PF_6$ at 4.5 GPa, a coupling that is weakly enhanced by CDW correlations according to X-ray experiments in selenide compounds [10]. If this coupling is singled out in perturbation theory an instability of the normal state towards a *s*-wave superconducting ordering will occur at best at $T_c \sim \omega_D \exp(-1/|g_{ph}|) \sim 100\exp(-20)$ K, which is vanishingly small. The prognostication is even worse for inter-chain pairing induced by phonons since the relevant coupling $g_{ph}^\perp \sim (t_\perp/t_a)^2 g_{ph}$ is reduced by a factor 100.

Arguments against the participation of phonons in superconductivity can be further sharpened if we consider that in the temperature domain below ω_D (~ 100 K) [49], exchange of phonons leads to essentially unretarded attractive interaction g_{ph} between electrons which simply adds to the Coulomb repulsion $[g_\mu(\ell_{\omega_D}) \rightarrow g_\mu^*(\ell_{\omega_D}) + g_{ph}(\ell_{\omega_D})]$. An overcome of g_μ^* by g_{ph} would then show up as a gradual freezing out of spin degrees of freedom which is not corroborated by experiments even in the close vicinity of T_c [50]. A similar argumentation also applies at much higher temperature when molecular phonons ($\omega_D \sim 1000$ K) are taken into account.

The coupling of electrons to $2k_F$ acoustic phonons, though singularly enhanced on the SP side by strong electronic correlations in the vertex part [46,47], becomes quickly non singular as the sequence of states unfolds under pressure − as confirmed by X-ray diffuse scattering experiments showing very weak, nearly inexistent, lattice precursors in the normal phase of $(TMTSF)_2X$ [10,51]. It is worthwhile to mention, however, that a recent re-examination of the X-ray data revealed that CDW and SDW ordering do coexist in few systems, $(TMTSF)_2PF_6$ being one example at ambient pressure [51–53]. Numerical simulations on 1D models indicate that coupling of electrons to phonons would be involved in this coexistence [54,55], though purely electronic models have been proposed [56]. On experimental grounds this CDW instability is apparently not the result of a soft mode mechanism that can lead to a strong renormalization of the electron-phonon matrix element in the normal phase [51].

3.4 Discussion

A conventional electron-phonon mechanism seems not appropriate to explain the pressure-induced superconductivity in $(TMTTF)_2PF_6$ at temperatures of the order of 2 K and therefore other approaches have to be considered. The correlation between the T_c-value and the width in temperature of the (insulating) spin-fluctuation regime is taken as a strong experimental argument in favour of a pairing mechanism involving AF fluctuations. Furthermore, the maximum value of T_c is about twice as large in $(TMTTF)_2PF_6$ as in the parent selenium compound [25] which is in agreement with the larger AF fluctuation regime observed in our investigation. This supports the idea that AF fluctuations are involved in the microscopic pairing mechanism similar to the scenario proposed for Ce- and U-based strongly correlated electron multiband systems [57,58].

SDW fluctuations have been considered by Emery [22] as another possibility to form bound states of charge carriers. This idea was worked out in the context of nearly AF itinerant fermion systems [23]. As far as 1D organic conductors are concerned, it was shown that the exchange of SDW fluctuations between carriers belonging to the same stack does not lead to attractive pairing and thus, the development of a 1D attractive pairing appears to be hopeless. Additionally, in 1D systems the electron-phonon coupling is opposed to the Coulomb repulsion of carriers moving in a restricted phase space.

In a conventional approach, using the spin fluctuation exchange model in quasi-1D organic superconductors, *d*-wave pairing in the vicinity of the SDW phase has been predicted [39]. This theory, however, does not take fully into account the entire temperature regime and in particular the non-Fermi-liquid features, observed in DC transport [17,59] and optical conductivity [15] at high temperature, which persist down to low temperature. As explained in detail in Section 3, an attractive inter-stack pairing can be the outcome of the exchange of AF spin fluctuations between electrons located on neighbouring stacks [37]. This would lead to an anisotropic superconducting gap. An inescapable prediction of scaling theory is that within the

framework of the low-energy quasi-1D model given by the effective Hamiltonian (1), singlet superconductivity is by far the most stable pairing state SDW fluctuations can stabilize giving in turn support for such an order parameter. Triplet pairing − which has been recently considered on both experimental and theoretical basis as a possible candidate for the superconducting state in the Bechgaard salts [50,60–65] − does exist in the present model between electrons on *next* to nearest-neighbour chains, but its enhancement is vanishingly small compared to singlet pairing [21]. In a model for superconductivity, based on an inter-chain attractive pairing, the existence of lines of nodes in the superconducting gap should be a natural outcome. Consequently, low lying quasi-particle states would govern the thermodynamical properties of the superconducting phase. Experiments such as thermal conductivity, sound attenuation or nuclear spin lattice relaxation should be able to probe this assumption. These measurements should however, be performed on a compound such as $(TMTSF)_2PF_6$ in which no additional anion ordering is likely to spoil the quasi-1D Fermi surface at low temperature [2,61].

4 Conclusion

We have reported pressure-induced superconductivity in $(TMTTF)_2PF_6$ *in spite of* its SP ground state at ambient pressure. This important result establishes the universality of the $(TM)_2X$ phase diagram with a single compound spanning all possible ground states of the $(TM)_2X$ series. Furthermore, the suppression of the SP ground state makes a phonon-mediated Cooper-pair formation unlikely to explain the existence of superconductivity at temperatures as high as $T_c = 2.2$ K at 4.73 GPa. The manifestation of critical SDW fluctuations above the onset of superconductivity and the close connection between their amplitude and the value of T_c speaks strongly in favour of an inter-stack pairing mechanism mediated by the exchange of these fluctuations between neighbouring stacks. Although the outcome of the phase diagram in the present weak coupling scheme cannot pretend to be quantitative, especially in the crossover region where strong coupling and dynamical effects are expected, one-loop scaling theory gives a fair account of many observed features and provides significant weight to the hypothesis of interfering channels in the emergence of superconductivity. Thus, our findings supply an important input for theoretical models of magnetic coupling in quasi-1D conductors and may even shed light on superconductivity in strongly correlated electron systems including high-temperature superconductors.

Useful discussions with C. Pasquier and P. Auban-Senzier as well as the technical help of M. Nardone are acknowledged. The work carried out in Geneva was supported by the Swiss National Science Foundation. We thank R. Cartoni and A. Holmes for technical assistance. C.B thanks L.G. Caron, N. Dupuis and A.-M. Tremblay for key discussions at the various stages of this work. C.B and R.D also thank the Natural Sciences and Engineering Research Council of Canada (NSERC), le Fonds pour la Formation de Chercheurs et l'Aide à la Recherche du Gouvernement du Québec (FCAR), the 'superconductivity program' of the Institut Canadien de Recherches Avancées (CIAR) for financial support.

References

1. D. Jérome, A. Mazaud, M. Ribault, K. Bechgaard, J. Phys. Lett. France **41**, L95 (1980).
2. C. Bourbonnais, D. Jérome, in *Advances in Synthetic Metals, Twenty Years of Progress in Science and Technology*, edited by P. Bernier, S. Lefrant, G. Bidan (Elsevier, New York, 1999) pp. 206–261.
3. V.J. Emery, R. Bruisma, S. Barisic, Phys. Rev. Lett. **48**, 1039 (1982).
4. L.G. Caron, C. Bourbonnais, Physica B **143**, 453 (1986).
5. S. Brazovskii, Y. Yakovenko, JETP **62**, 1340 (1985).
6. C. Bourbonnais, in *Strongly interacting fermions and high-T_c superconductivity, Session LVI (1991), Les Houches*, edited by B. Doucot, J. Zinn-Justin (Elsevier Science, Amsterdam, 1995) pp. 307–367.
7. C. Bourbonnais, D. Jérome, Science **281**, 1156 (1998).
8. C. Coulon, P. Delhaes, S. Flandrois, R. Lagnier, E. Bonjour, J.M. Fabre, J. Phys. France **43**, 1059 (1982).
9. R. Brusetti, M. Ribault, D. Jérome, K. Bechgaard, J. Phys. France **43**, 801 (1982).
10. J.P. Pouget, R. Moret, R. Comes, K. Bechgaard, J.M. Fabre, L. Giral, Mol. Cryst. Liq. Cryst. **79**, 129 (1982).
11. F. Creuzet, S.S.P. Parkin, D. Jérome, J.M. Fabre, J. Phys. Colloq. France **44**, 1099 (1983).
12. P. Wzietek, F. Creuzet, C. Bourbonnais, D. Jérome, K. Bechgaard, P. Batail, J. Phys. I France **3**, 171 (1993).
13. L. Balicas, K. Behnia, W. Kang, E. Canadell, P. Auban-Senzier, D. Jérome, M. Ribault, J.M. Fabre, J. Phys. I France **4**, 1539 (1994).
14. B.J. Klemme, S.E. Brown, P. Wzietek, G. Kriza, P. Batail, D. Jérome, J.M. Fabre, Phys. Rev. Lett. **75**, 2408 (1995).
15. V. Vescoli, L. Degiorgi, W. Henderson, G. Gruner, K.P. Starkey, L.K. Montgomery, Science **281**, 1181 (1998).
16. D.S. Chow, P. Wzietek, D. Foglatti, B. Alavi, D.J. Tantillo, C.A. Merlic, S.E. Brown, Phys. Rev. Lett. **81**, 3984 (1998).
17. J. Moser, M. Gabay, P. Auban-Senzier, D. Jérome, K. Bechgaard, J.M. Fabre, Eur. Phys. J. B **1**, 39 (1998).
18. D.S. Chow, F. Zamborszky, B. Alavi, D.J. Tantillo, A. Baur, C.A. Merlic, S.E. Brown, Phys. Rev. Lett. **85**, 1698 (2000).
19. D. Jaccard, H. Wilhelm, D. Jérome, J. Moser, C. Carcel, J.M. Fabre, J. Phys. Cond. Matt. **13**, L89 (2001); `cond-mat/0005378`.
20. In the course of writting this manuscript our experimental results have found additional support by similar findings reported by T. Adachi, E. Ojima, K. Kato, H. Kobayashi, T. Miyazaki, M. Tokumoto, A. Kobayashi, J. Am. Chem. Soc. **122**, 3238 (2000).
21. R. Duprat, C. Bourbonnais, `cond-mat/0102139`.
22. V.J. Emery, Synthetic Metals **13**, 21 (1986).

23. M.T. Béal-Monod, C. Bourbonnais, V.J. Emery, Phys. Rev. B **34**, 7716 (1986).
24. D. Jaccard, E. Vargoz, K. Alami-Yadri, H. Wilhelm, Rev. High Pressure Sci. Technol. **7**, 412 (1998).
25. D. Jérome, H.J. Schulz, Adv. Phys. **31**, 299 (1982).
26. L.J. Azevedo, J.E. Schirber, J.M. Williams, M.A. Beno, D.R. Stephens, Phys. Rev. B **30**, 1570 (1984).
27. M. Héritier, G. Montambaux, P. Lederer, J. Phys. Lett. France **45**, L943 (1984).
28. G. Montambaux, in *Low Dimensional Conductors and Superconductors*, edited by D. Jérome, L.G. Caron (Plenum Press, New York, 1987), p. 233.
29. D. Jérome, in *Organic Conductors: fundamentals and applications*, edited by J.-P. Farges (Dekker, New York, 1994), p. 405.
30. P.M. Grant, J. Phys. Colloq. France **44**, 847 (1983).
31. K. Behnia, L. Balicas, W. Kang, D. Jérome, P. Carretta, Y. Fagot-Revurat, C. Berthier, M. Horvatic, P. Ségransan, L. Hubert, C. Bourbonnais, Phys. Rev. Lett. **74**, 5272 (1995).
32. C. Bourbonnais, L.G. Caron, Int. J. Mod. Phys. B **5**, 1033 (1991).
33. T. Ishiguro, K. Yamaji, in *Organic Superconductors* (Springer, Berlin, Springer Series in Solid-State Science, 1990), Vol. 88.
34. K. Yamaji, J. Phys. Soc. Jpn **51**, 2787 (1982).
35. Chr. Seidel, V.N. Prigodin, J. Phys. Lett. France **44**, L403 (1983).
36. Y. Hasegawa, H. Fukuyama, J. Phys. Soc. Jpn **56**, 877 (1987).
37. C. Bourbonnais, L.G. Caron, Europhys. Lett. **5**, 209 (1988).
38. H. Shimahara, J. Phys. Soc. Jpn **57**, 1044 (1988).
39. H. Kino, H. Kontani, J. Phys. Soc. Jpn **68**, 1481 (1999).
40. This variation includes the influence of Umklapp scattering which leads to a decrease of coupling constants with pressure that is more rapid than the one obtained from pure band effects.
41. F. Creuzet, C. Bourbonnais, L.G. Caron, D. Jérome, K. Bechgaard, Synthetic Metals **19**, 289 (1987).
42. J. Friedel, J. Phys. Lett. France **36**, L279 (1975).
43. K. Yamaji, J. Phys. Soc. Jpn **52**, 1361 (1983).
44. V.Z. Kresin, H. Morawitz, S.A. Wolf, in *Mechanisms of conventional and high T_c superconductivity* (Oxford University Press, New York, 1993).
45. M. Dumm, A. Loidl, B. Fravel, K.P. Starkey, L.K. Montgomery, M. Dressel, Phys. Rev. B **61**, 511 (2000).
46. L.G. Caron, C. Bourbonnais, F. Creuzet, D. Jérome, Synthetic Metals **19**, 69 (1987).
47. C. Bourbonnais, B. Dumoulin, J. Phys. I France **6**, 1727 (1996).
48. F. Castet, A. Fritsch, L. Ducasse, J. Phys. I France **6**, 583 (1996).
49. P. Garoche, R. Brusetti, K. Bechgaard, Phys. Rev. Lett. **49**, 1346 (1982).
50. I.J. Lee, D.S. Chow, W.G. Clark, M.J. Strouse, M.J. Naughton, P.M. Chaikin, `cond-mat/0001332`.
51. J.P. Pouget, S. Ravy, J. Phys. I France **6**, 1501 (1996).
52. J.P. Pouget, J. Phys. IV France **61**, Pr3-43 (2000).
53. S. Kagoshima, Solid State Commun. **110**, 479 (1999).
54. S. Mazumdar, R. Ramasesha, R. Torsen Clay, D.K. Campbell, Phys. Rev. Lett. **82**, 1522 (1999).
55. J. Riera, D. Poilblanc, Phys. Rev. B **62**, R16243 (2000); `cond-mat/0006460`.
56. M. Ogata, N. Kobayashi, K. Yonemitsu, Synthetic Metals **103**, 2242 (1999).
57. S.R. Julian, C. Pfleiderer, F.M. Grosche, N.D. Mathur, G.J. McMullan, A.J. Diver, I.R. Walker, G.G. Lonzarich, J. Phys. Cond. Matt. **8**, 9675 (1996); N.D. Mathur, F.M. Grosche, S.R. Julien, I.R. Walker, D.M. Freye, R.K.W. Haselwimmer, G.G. Lonzarich, Nature **394**, 39 (1998).
58. M. Jourdan, M. Huth, H. Adrian, Nature **398**, 47 (1999).
59. G.M. Danner, W. Kang, P.M. Chaikin, Phys. Rev. Lett. **72**, 3714 (1994).
60. L.P. Gorkov, D. Jérome, J. Phys. Lett. **46**, L643 (1985).
61. S. Belin, K. Behnia, Phys. Rev. Lett. **79**, 2125 (1997).
62. I.J. Lee, M.J. Naughton, G.M. Danner, P.M. Chaikin, Phys. Rev. Lett. **78**, 3555 (1997).
63. A.G. Lebed, JETP Lett. **44**, 114 (1986).
64. N. Dupuis, G. Montambaux, C.A.R. Sá de Melo, Phys. Rev. Lett. **70**, 2613 (1993).
65. A.G. Lebed, Phys. Rev. B **59**, R721 (1999).